# AGN – Physics of the Ionized Gas

- Physical conditions in the NLR
- Physical conditions in the BLR
- LINERs
- Emission-Line Diagnostics
- High-Energy Effects

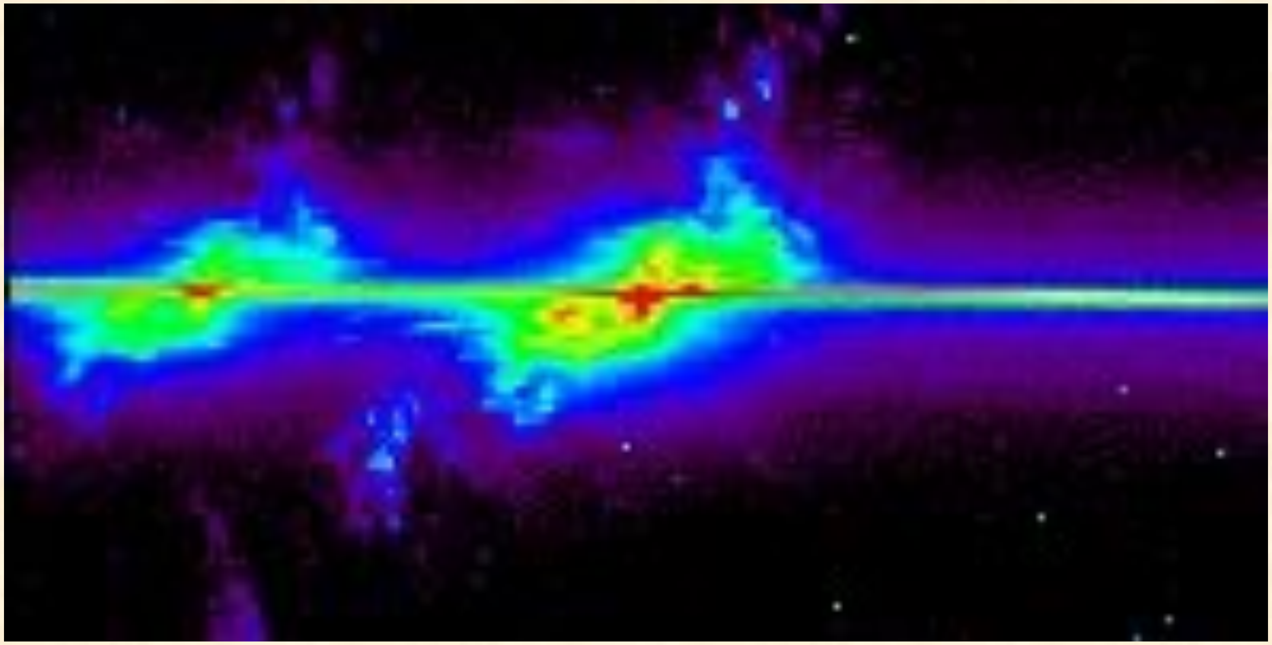

# Evidence for Photoionization

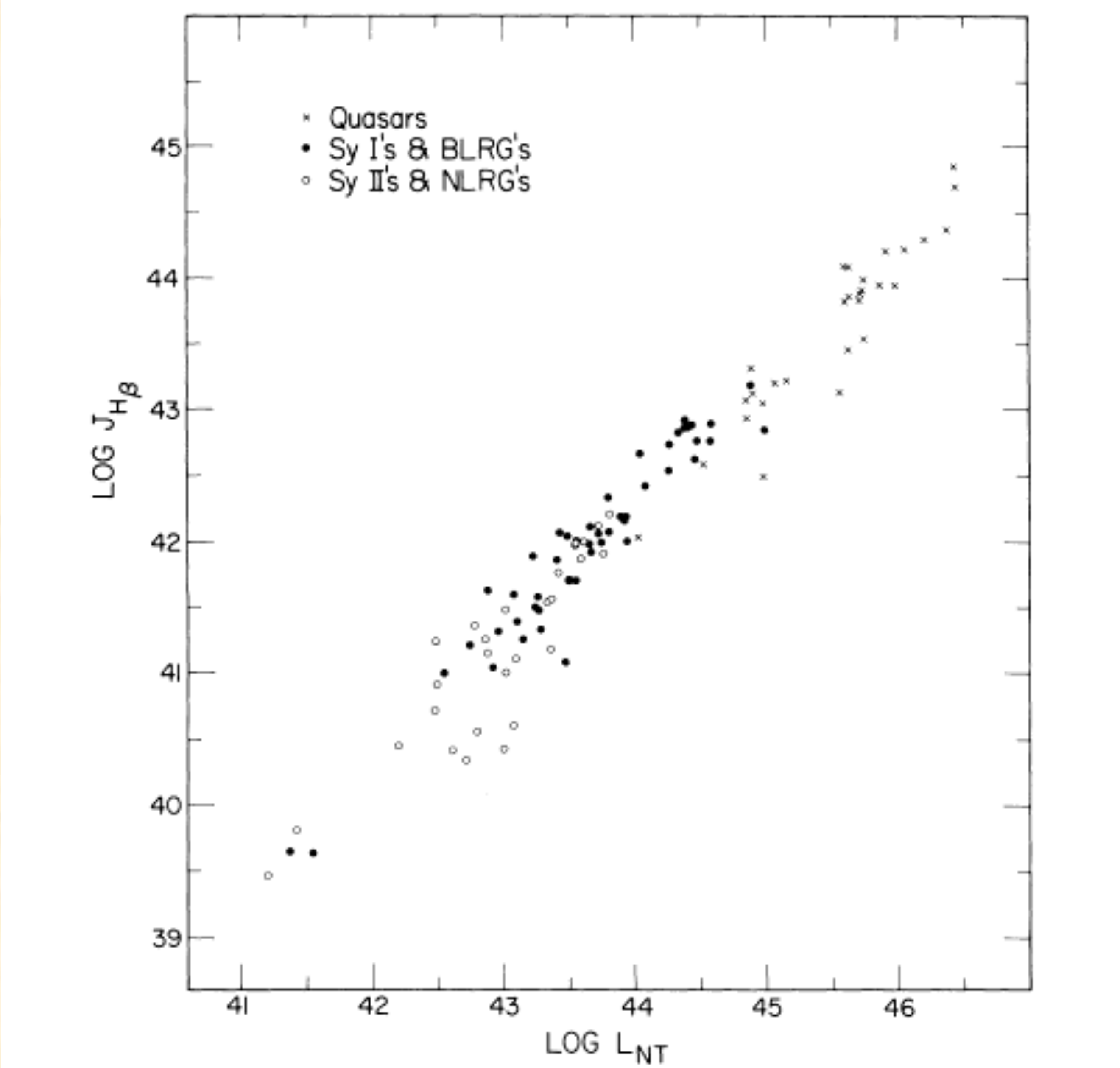


- continuum and Hβ luminosity correlated over a huge range

(Yee, H. 1980, ApJ, 241, 894)

# Emission-Line Diagnostics for Seyfert NLRs

- T = 10,000 – 20,000 K from [O III] lines → photoionization (shock heating gives temperatures ≈ 40,000 K)
- Emission lines span a wide range in ionization potential (IP):

  - IP needed to create [O I]: 0 eV, [Fe X IV]: 361 eV

  → Power-law SEDs with substantial X-ray contribution
- UV radiation forms a classic H II region on the "front face"
- X-rays penetrate deep into the cloud to create a "partially-ionized zone" (PIZ): N(H II)/N(H I) ≈ 0.1 to 0.2
  - In the PIZ, elements are neutral or singly ionized
  - substantial emission from HI, [O I], [N II], [S II], Mg II

  → Large column densities ($N_H = 10^{19} – 10^{21}$ cm$^{-2}$)
- HST resolved spectroscopy shows wide range in number density.

  → $n_H = 10^2 - 10^7$ cm$^{-3}$ (from lines with a range in critical density)

# Collisional Excitation of H Lines in the PIZ

- X-rays penetrate deep into the cloud to create high-energy ("suprathermal") electrons, which cause multiple ionizations in the mostly neutral gas.
- Suprathermal electrons also collisionally excite the n = 1 level in hydrogen:
- Lα is collisionally enhanced relative to the other H lines

$$4\pi j_\nu = n_e n_{H^0} q_{12} h\nu_{L\alpha}$$ , where q is the collision rate

- Lα/Hβ can reach ~50 in the NLR, compared to recombination value of 33.
- Hα is the next most collisionally enhanced line (n = 1 to n = 3)
- Hα/Hβ can reach ~ 3.1 in the NLR, compared to the recombination value of ~2.85

# Results from NLR models

- Photoionization codes like CLOUDY contain all of the important physics (X-ray ionization of the PIZ, collisional excitation and ionization, Auger effect, charge exchange, etc.)
- Input parameters: U (or luminosity and distance for spatially resolved regions), continuum shape (SED), number density ($n_H$), abundances, column densities ($N_H$).
- Models indicate abundances are approximately solar
  - previous "low abundance" cases due to a high-density component, which suppresses the forbidden lines (CNO, etc.)
- Multiple components (with different U, $n_H$) are usually needed at each position.
- Power-law interpolation between UV and X-ray ($\alpha_\nu \approx 1.5$) works - no need for huge EUV bump (BBB)
- Dust within the clouds can suppress resonance lines (esp. Ly$\alpha$)

# Ex) STIS Long-Slit Spectra of the NLR in NGC 4151

(Kraemer et al. 2000, ApJ, 531, 278)

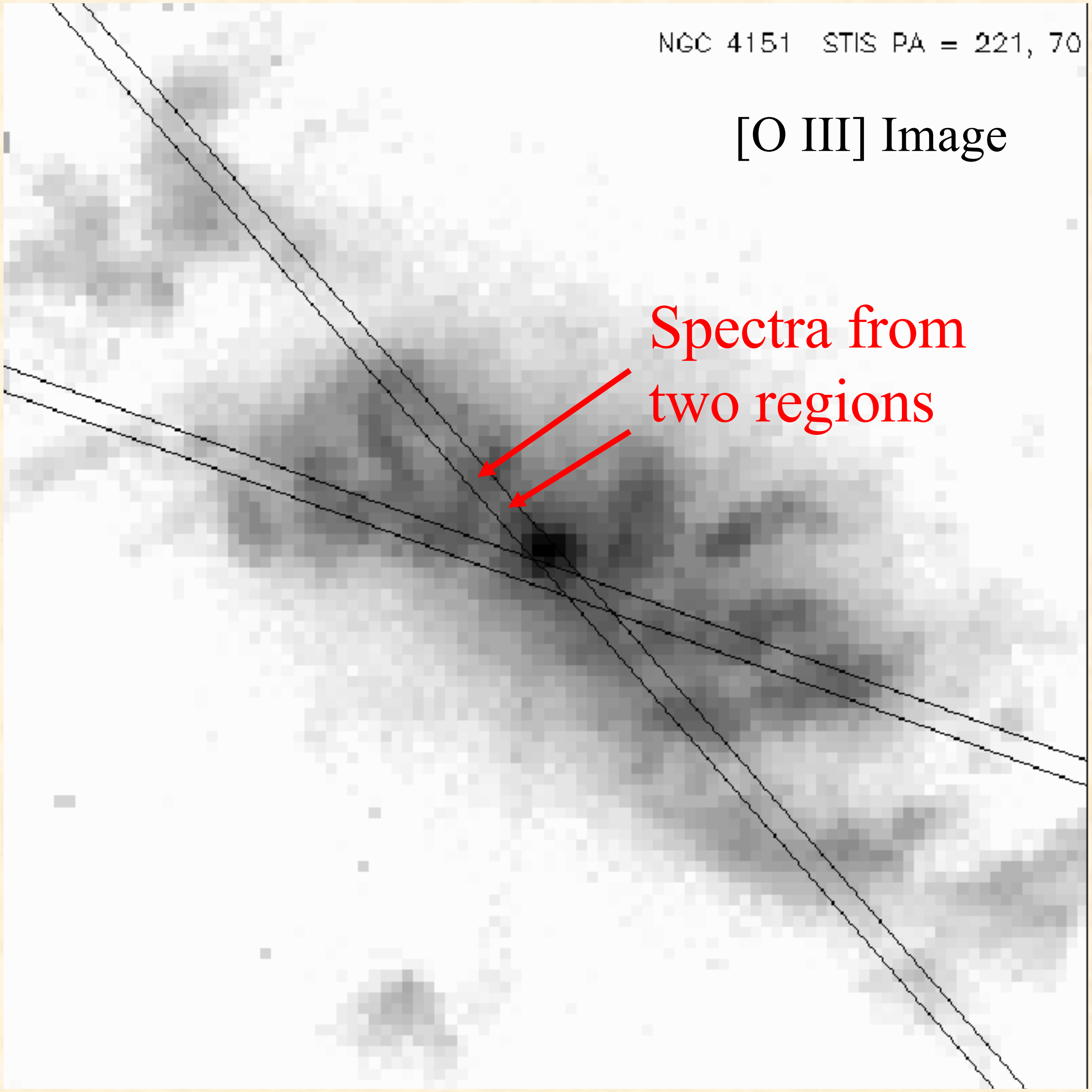

# Model Results from Two Regions

| Spectral Bin | Log U | $n_e$ ($cm^{-3}$) | $N_H$($cm^{-3}$) | % Hβ | Note |
|---|---|---|---|---|---|
| 0.1-0.3 NE | -2.67 | 1.2 E4 | 1.6 E 21 | 50% | RB |
| | -3.0 | 1.0 E7 | 5.6 E 19 | 25% | MB |
| | -1.08 | 1.0 E5 | 5.6 E 20 | 25% | MB |
| 0.3-0.5 NE | -2.67 | 1.2 E4 | 1.6 E21 | 90% | RB |
| | -1.36 | 6.0 E2 | 5.3 E 20 | 10% | MB |

MB – matter bounded (optically thin)

RB – radiation bounded (optically thick)

# Comparison of Models and Observations

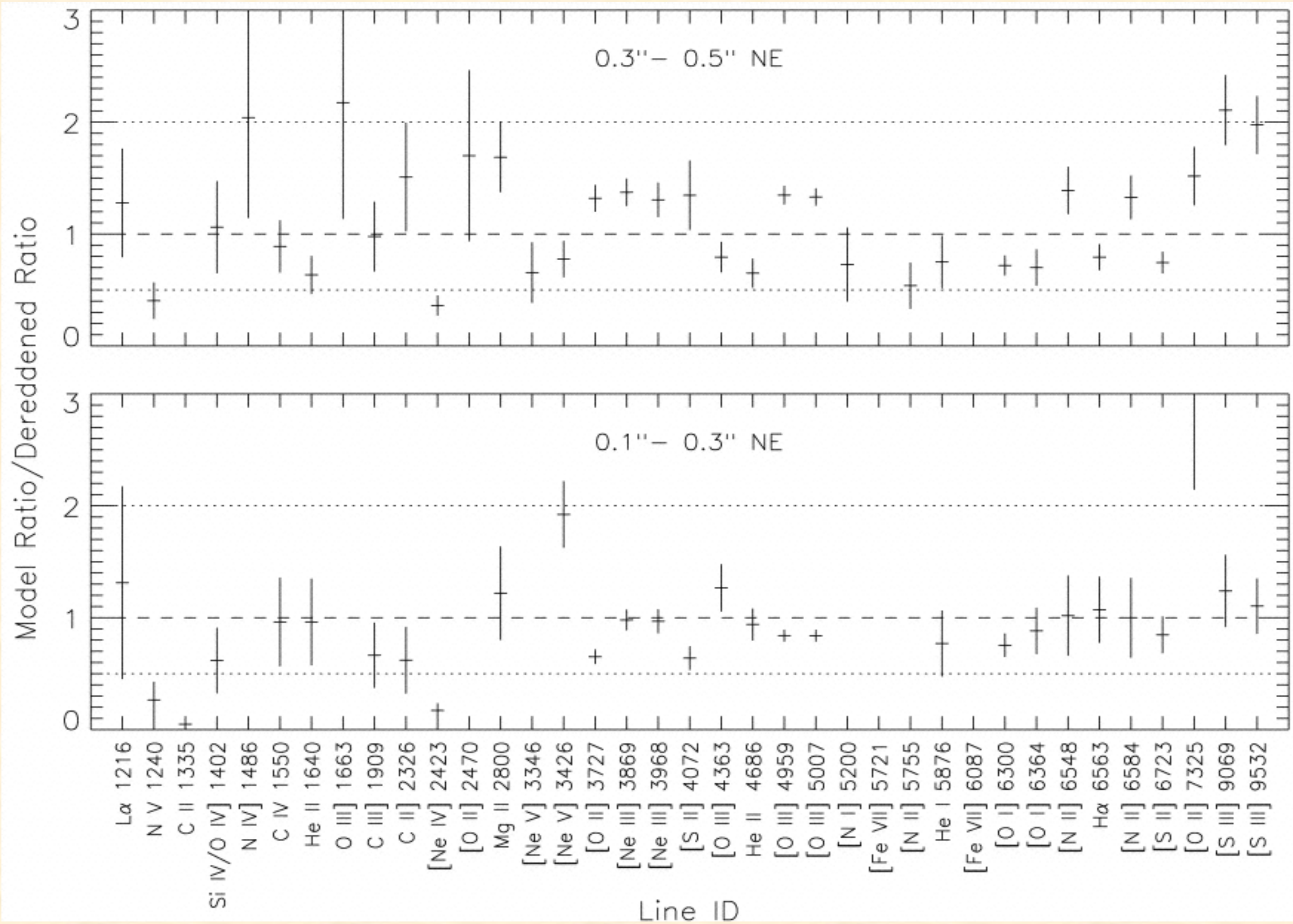

# Physical Diagnostics of the BLR

- No forbidden lines, some semi-forbidden lines:
  - No broad [O III] $\lambda\lambda$4959, 5007 → $n_H \geq 10^8$ cm$^{-3}$
  - Broad C III] $\lambda$1909: → $n_H \leq 10^{11}$ cm$^{-3}$
- Cooling is primarily done by recombination lines (H and He) and collisional excitation of permitted lines (e.g., C IV, N V in UV; Fe II in UV and optical)
- X-ray ionization (also important in NLR)

  - ejected outer shell (suprathermal) electrons causes ~6 collisional ionizations

  - Auger effect: X-ray photon can eject multiple electrons

$$\text{Ex) } O^{+2}(1s^2 2s^2 2p^2\ ^3P) + h\nu \rightarrow O^{+3}(1s\ 2s^2 2p^2\ ^2P) + e^-$$

– leaves $O^{+3}$ in excited state

$$O^{+3}(1s\ 2s^2 2p^2\ ^2P) \rightarrow O^{+4}(1s^2 2s^2\ ^1S) + e^- \text{ (autoionization)}$$

- Fe II, Mg II, C I, and O I are enhanced in the PIZ → $N_H = 10^{22} - 10^{23}$ cm$^{-2}$
- BLR is not resolved: $U = 10^{-2}$ to $10^{-1}$ from photoionization models
- Dust cannot survive in the BLR. Seyferts have "normal" abundances

# The "Lα/Hβ" Problem

- Baldwin (1977) discovered the "Lα/Hβ" problem by piecing together spectra of QSOs at different redshifts
  - Lα/Hβ ≈ 5 – 10 for the BLR, whereas recombination gives ~33
  - What's going on?
- BLR clouds have large column and number densities.
- Lα scatters throughout the PIZ in BLR clouds, populating the n = 2 level
- Hβ (and Hα) are collisionally excited in the PIZ, and therefore enhanced by factors of 3 – 6 over recombination values
- Lα is further reduced by ionization of electrons in n = 2 level
- Currently, there is still an "Fe II" problem: models underpredict the amount of Fe II emission
  - huge number of levels, so radiative transfer (radiative pumping, resonance fluorescence, and transition coincidences) and collisional excitations are complicated

# Fe II Partial Grotrian Diagram

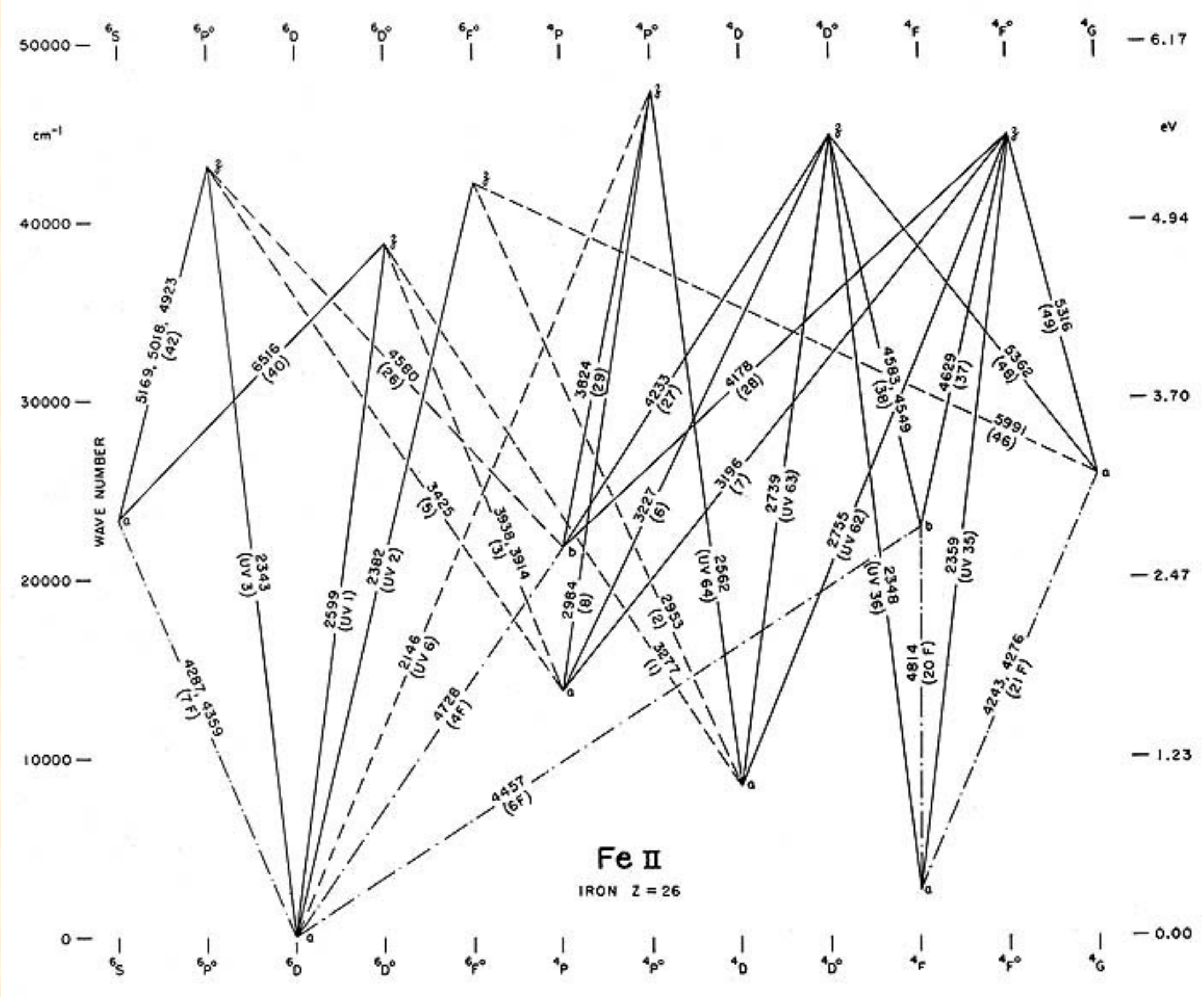

# BLR "Cloud" Photoionization Model

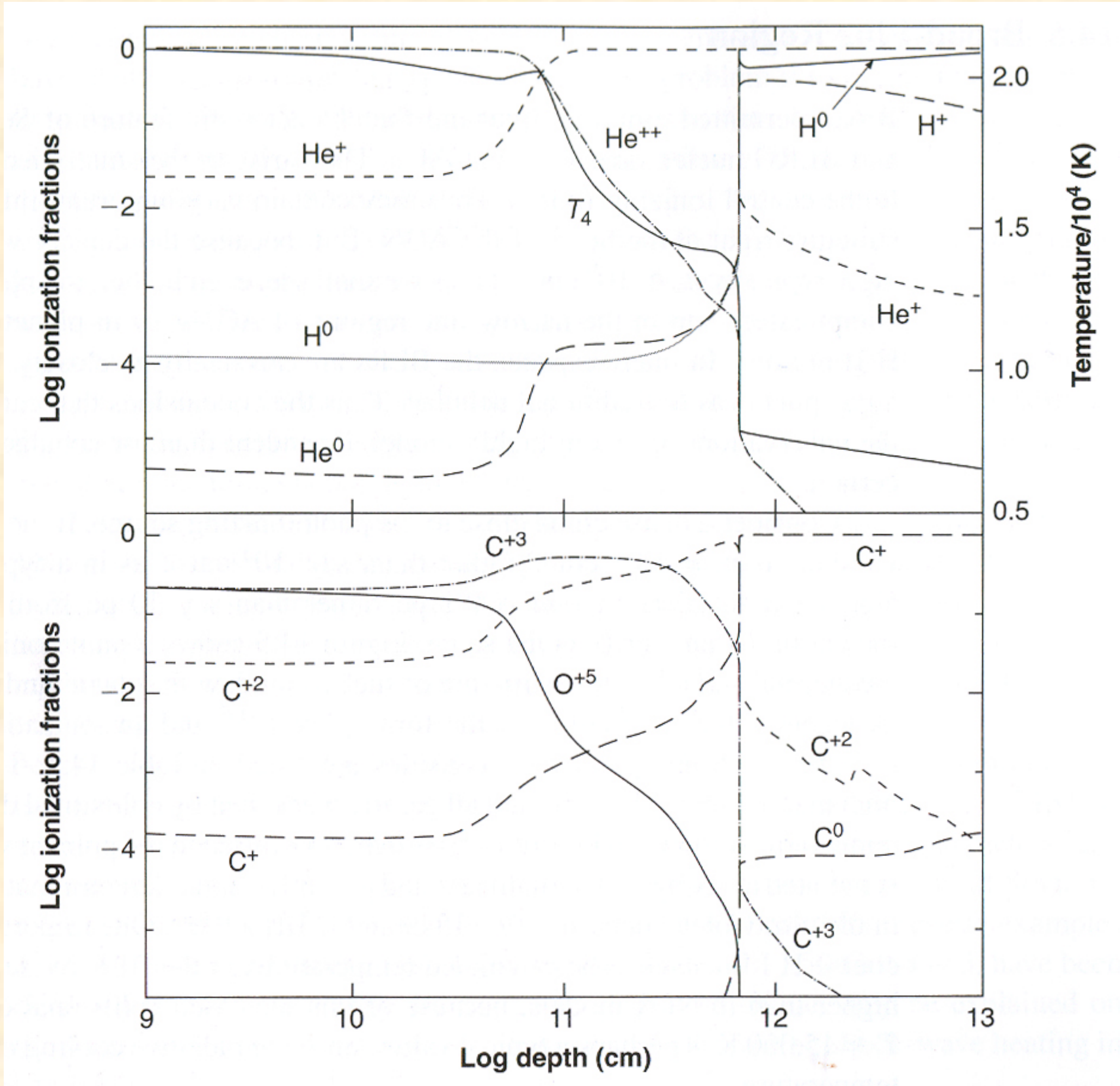


(Osterbrock & Ferland, p. 364)

# BLR Line Ratios

Observed and predicted relative BLR emission-line intensities

| Ion | $\lambda$ (Å) | Observed[a] | $U = 10^{-1.5}$ Model | Multi-component Model |
|---|---|---|---|---|
| O VI | 1034 | 0.1–0.3 | 0.019 | 0.16 |
| L$\alpha$ | 1216 | 1.00 | 1.00 | 1.00 |
| N V | 1240 | 0.1–0.3 | 0.039 | 0.04 |
| Si IV + O IV | ~1400 | 0.08–0.24 | 0.091 | 0.06 |
| C IV | 1549 | 0.4–0.6 | 0.77 | 0.57 |
| He II + O III] | 1666 | 0.09–0.2 | 0.13 | 0.14 |
| C III] + Si III] | 1909 | 0.15–0.3 | 0.077 | 0.12 |
| Mg II | 2798 | 0.15–0.3 | 0.16 | 0.34 |
| H$\beta$ | 4861 | 0.07–0.2 | 0.045 | 0.09 |

a. The observed intensities from a sample of intermediate ($z \approx 2$) redshift quasars.

(Osterbrock & Ferland, p. 365)

- note: no prediction of Fe II emission … hmmm

# BLR Parameters from Photoionization Models

- Sizes: typically ~10 light days (in diameter) for Seyfert 1s

  1) Reverberation mapping – use time lag ($\tau$) of emission lines with respect to continuum variations: $r = c\tau$

  2) Photoionization models: Determine ionization parameter and density from models. Determine $Q_{ion}$ from luminosity and SED.

$$U = \frac{Q_{ion}}{4\pi r^2 c n_e} \rightarrow \text{solve for r.} \quad \text{To 1st order, } r \propto \sqrt{L}$$

- Mass of ionized gas in BLR:

$$L(H\beta) = n_e n_p \alpha^{eff}_{H\beta} h\nu_{H\beta} V\varepsilon \qquad \text{where } \varepsilon = \text{filling factor}$$

$$M_{BLR} \approx V\varepsilon n_p m_p = \frac{L(H\beta) m_p}{n_e \alpha^{eff}_{H\beta} h\nu_{H\beta}} \approx 0.7\ L_{42}(H\beta)\ \frac{10^{10}\,\text{cm}^{-3}}{n_e}\ M_\odot$$

- Filling factor $\varepsilon$: assume a spherical BLR ($V = \tfrac{4}{3}\pi r^3$)

$$\text{From above: } \varepsilon = \frac{L(H\beta)}{n_e n_p \alpha^{eff}_{H\beta} h\nu_{H\beta} V} \approx 0.01 - 0.1$$

- Covering factor – fraction of sky covered by BLR clouds
  - assume all ionizing photons are absorbed and use predicted equivalent width of emission line W(Hβ)

$$L_{H\beta} = h\nu_{H\beta} \frac{\alpha_{H\beta}^{eff}(H^0,T)}{\alpha_B(H^0,T)} \int_{\nu_0}^{\infty} \frac{L_\nu}{h\nu}\, d\nu$$

$$L_{H\beta} = L_\lambda(\lambda 4861) W_\lambda(H\beta) = L_\nu(\lambda 4861)\frac{d\nu}{d\lambda} W_\lambda(H\beta)$$

Assume power-law continuum: $L_\nu = C\nu^{-n}$

Then $W_\lambda(H\beta) = \dfrac{\lambda_{H\beta}}{n} \dfrac{\alpha_{H\beta}^{eff}(H^0,T)}{\alpha_B(H^0,T)} \left(\dfrac{\nu_0}{\nu_{H\beta}}\right)^{-n} = \dfrac{568}{n}(5.33)^{-n}$

( for a covering factor of 1)

So for $n = 1$, the predicted EW is $W_\lambda(H\beta) \approx 106$ Ang.

The covering factor is: $C_f = \dfrac{W_{obs}(H\beta)}{W_p(H\beta)} = \dfrac{20}{106} \approx 0.2$

# LINERs

- [O III]/Hβ < 3 (like galaxies with H II nuclei)
- [O I]/Hα > 0.05 (like the NLR in Seyferts)
- Original suggestion: shock heating or hot stars
- However, subsequent evidence indicates photoionization by AGN continuum (including X-rays) is likely for most
- $U = 10^{-3}$ to $10^{-5}$ for LINERs (rather than $10^{-1}$ to $10^{-2}$ for Seyferts)
- Probably due to low luminosity of continuum source, rather than higher density or greater distance

$$U = \frac{Q_{ion}}{4\pi r^2 c n_e}$$

- Further evidence for AGN: ~20% of LINERs show a mini BLR (type 1 LINERs)
- Transition objects: may be combination of starburst and AGN

# Emission-Line Diagnostics (BPT Diagram)

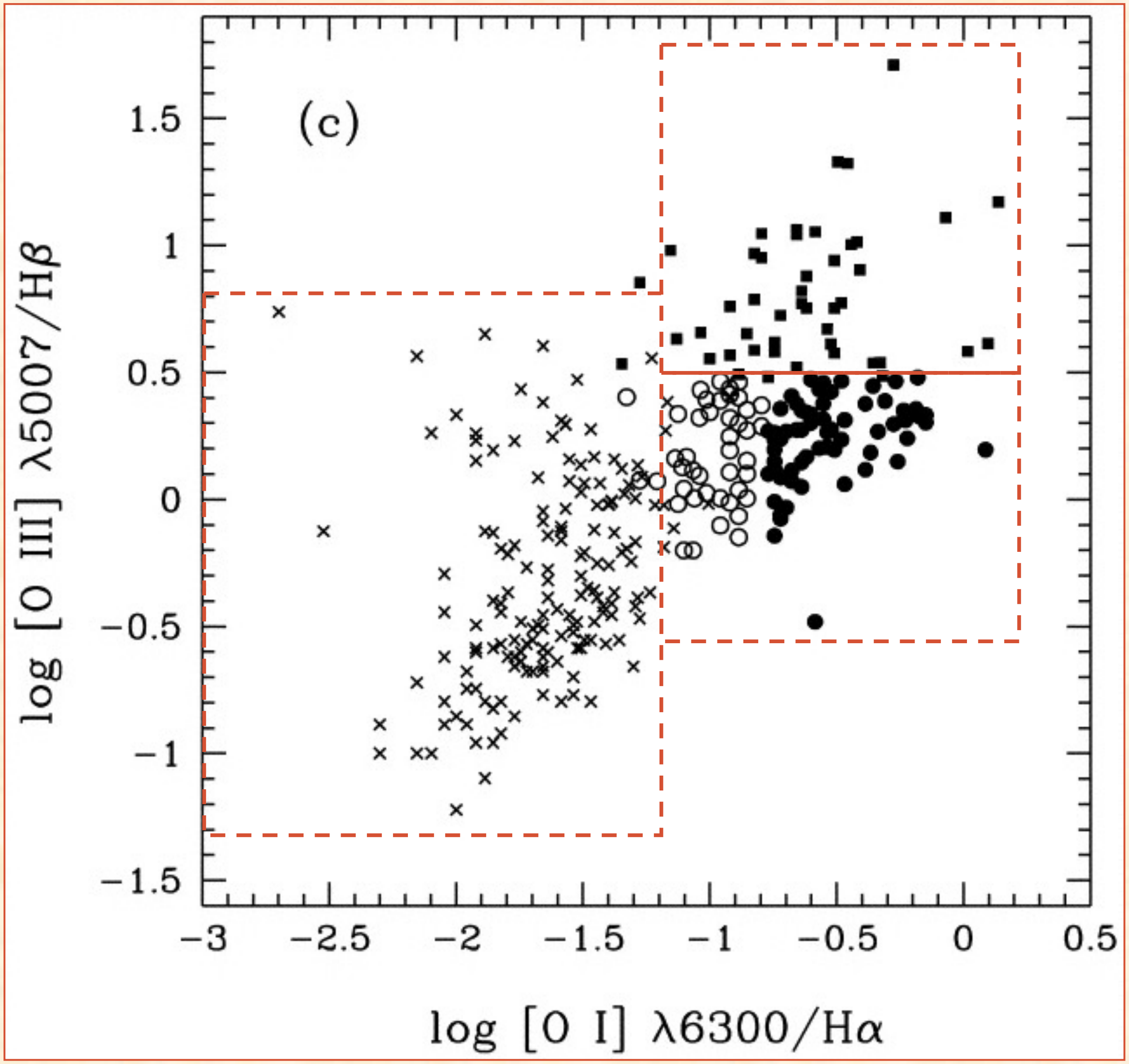


x - H II galaxy
■ - Seyfert NLR
● - “pure” LINER
○ - transition object (H II + LINER)

(Ho, Filippenko, & Sargent, 1997, ApJS 112, 315)

# Refined BPT Diagrams (85,000 galaxies from SDSS)

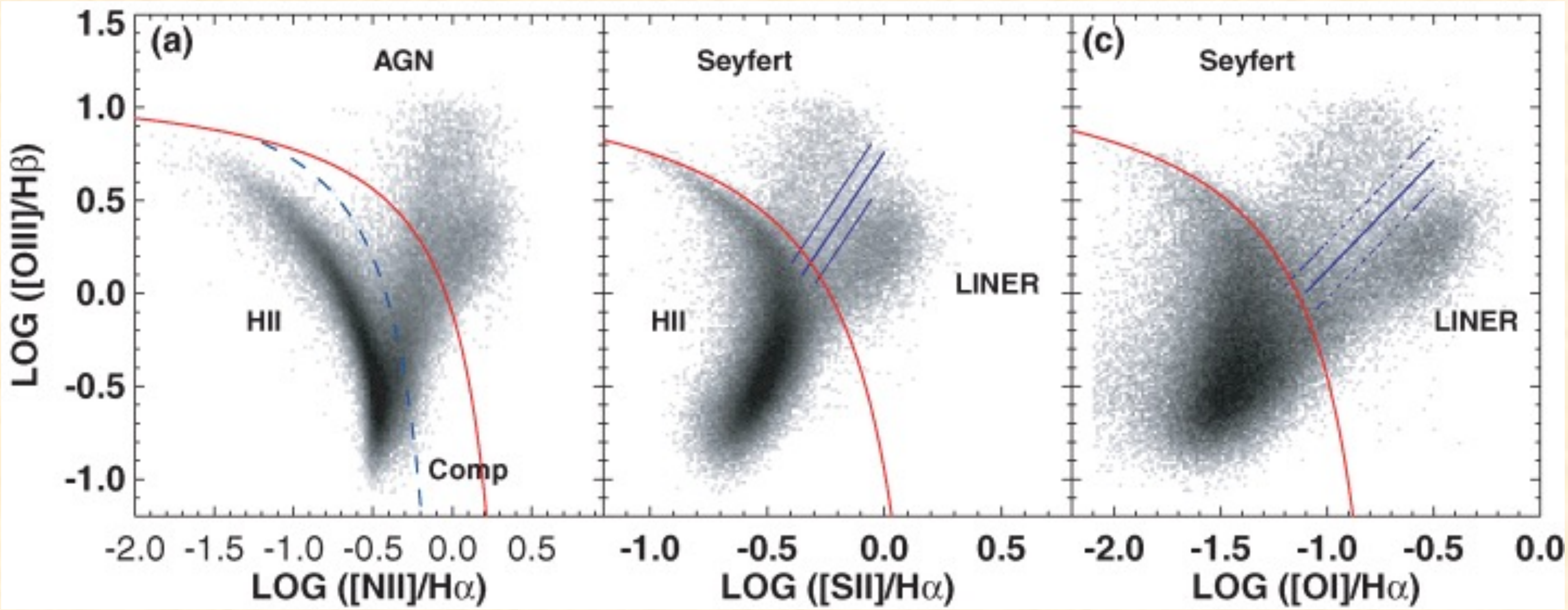


(Kewley et al. 2006, MNRAS, 372, 961 )

- H II (starburst) sequence from low to high metallicity (left to right)
- Composite ("transition") objects between blue and red lines in 1$^{st}$ figure
- Seyfert/LINER transition given as middle blue line in 2$^{nd}$ and 3$^{rd}$ figures (increasing ionization from lower right to upper left)

# High Energy Processes/ X-ray Spectra of AGN

- X-ray spectra of AGN show evidence for hot photoionized gas (T = 30,000 - 100,000 K; U = 1 - 10)
- Heating:
  - Photoionization of inner and outer shell electrons
  - Collisional ionization from ejected outer-shell (suprathermal) electrons
- Cooling:
  - Recombination lines: dominant in X-ray spectra (transitions to inner shells: n = 1,2,3 corresponding to K, L, M)
  - Fluorescence after ejection of inner-shell electrons: competes with Auger effect
  - Radiative recombination continuum (RRC), e.g., Lyman continuum (LC) : narrow, since $kT << I.P.$
  - Two-photon: significant, since critical density for 2s in H-like heavy elements is $> 10^{14}$ cm$^{-3}$.
  - Photoexcitation important due to many lines in spectra.
  - Collisional excitation: not so important in X-ray spectra: $kT << \chi$

# X-ray opacities

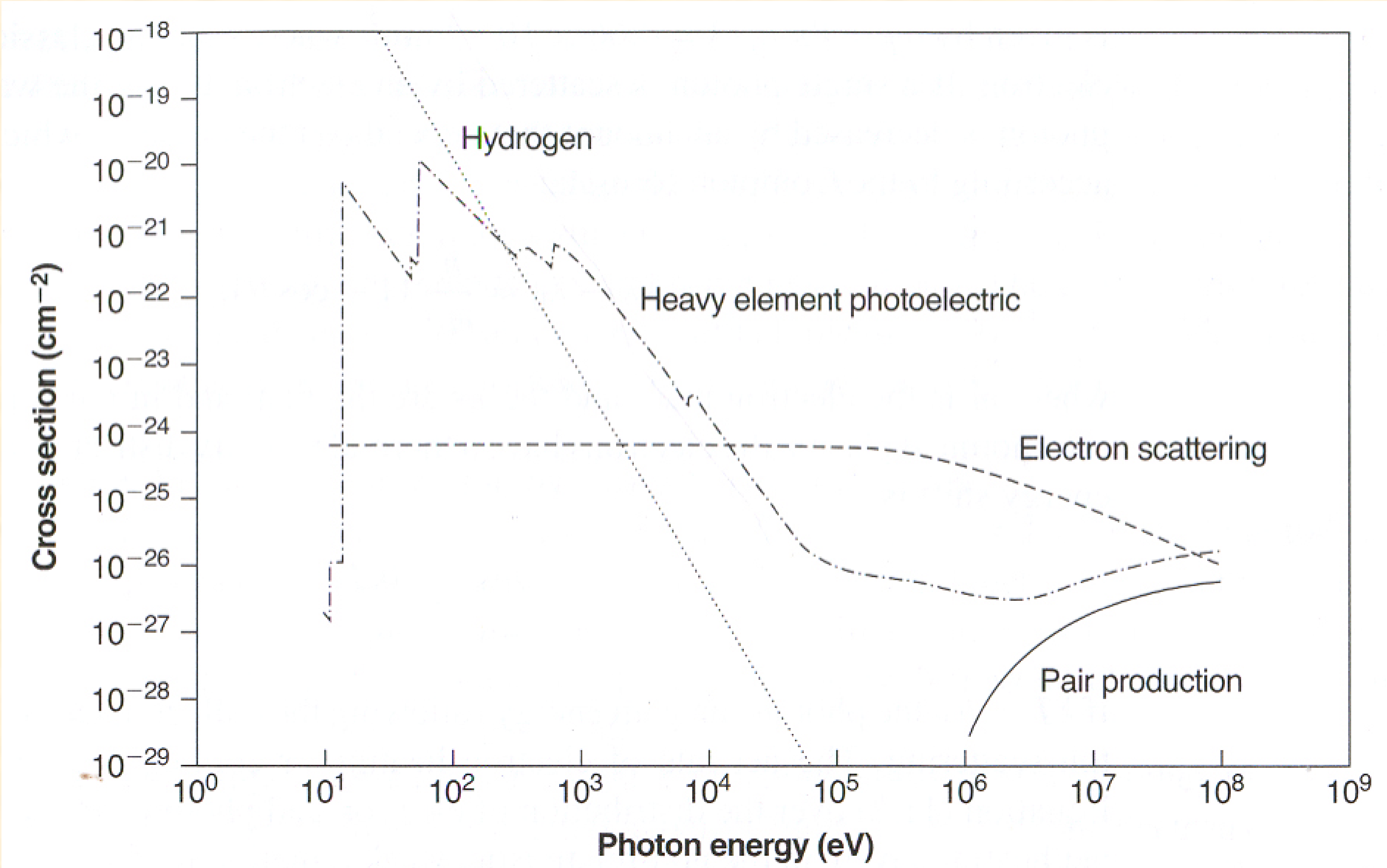


(Osterbrock & Ferland, p. 283)

- If seen in absorption , we can see the effects of absorption edges and scattering on the ionizing continuum: $\tau_\nu = a_\nu N_{ion}$
- The gas starts to become "Compton thick" at $N_e \sim 1/a_\nu \sim 10^{24}$ cm$^{-2}$

# Soft X-ray Emission-Line Spectra

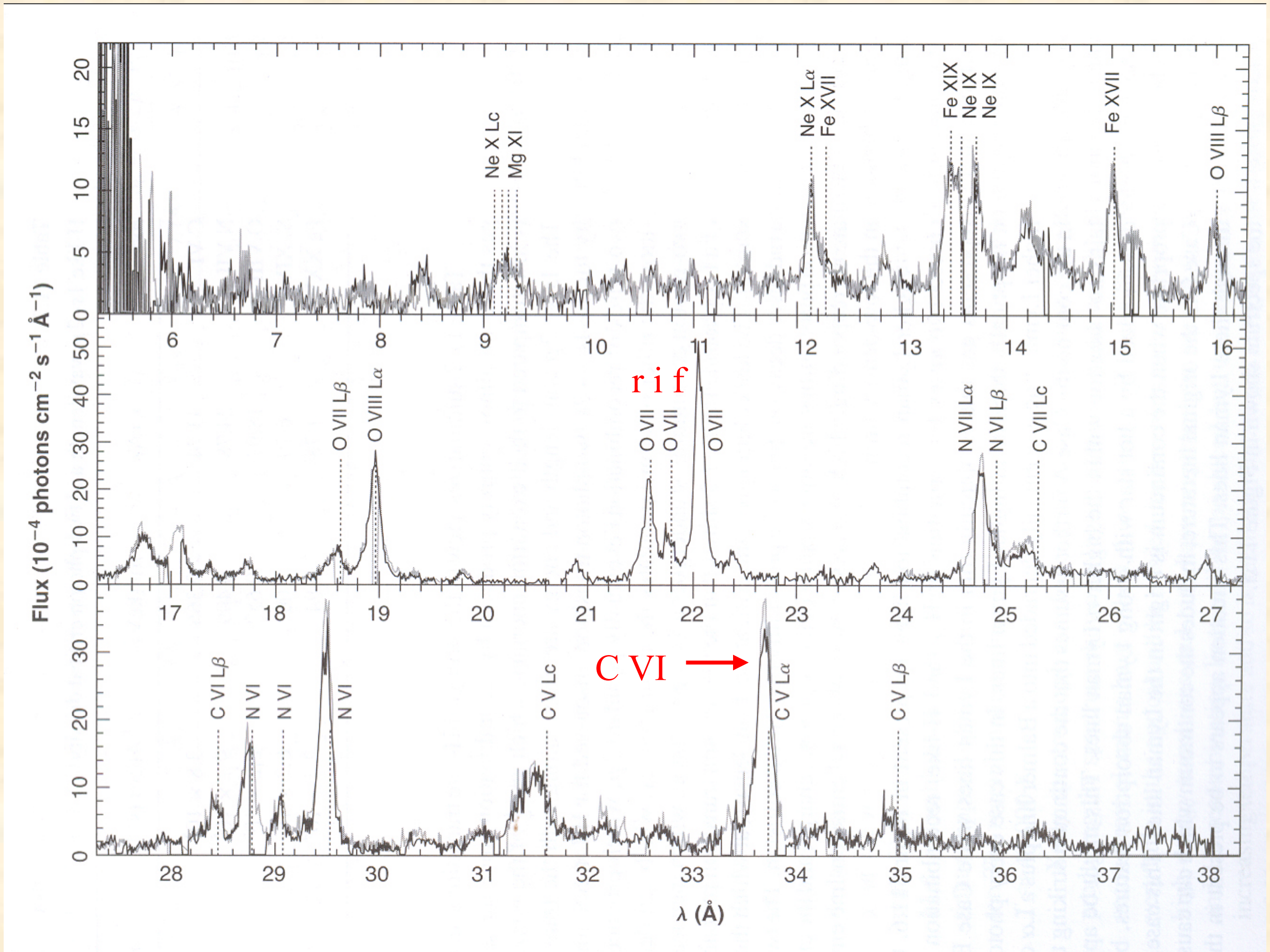


(Osterbrock & Ferland, p. 287)

- Chandra images reveal extended X-ray gas in the NLR of NGC 1068
- Chandra spectra reveal emission lines - mostly H and He-like.
- Observed lines can be matched by photoionization models with U ≈ 1 -10

# He-like Triplet Lines (rif): O VII

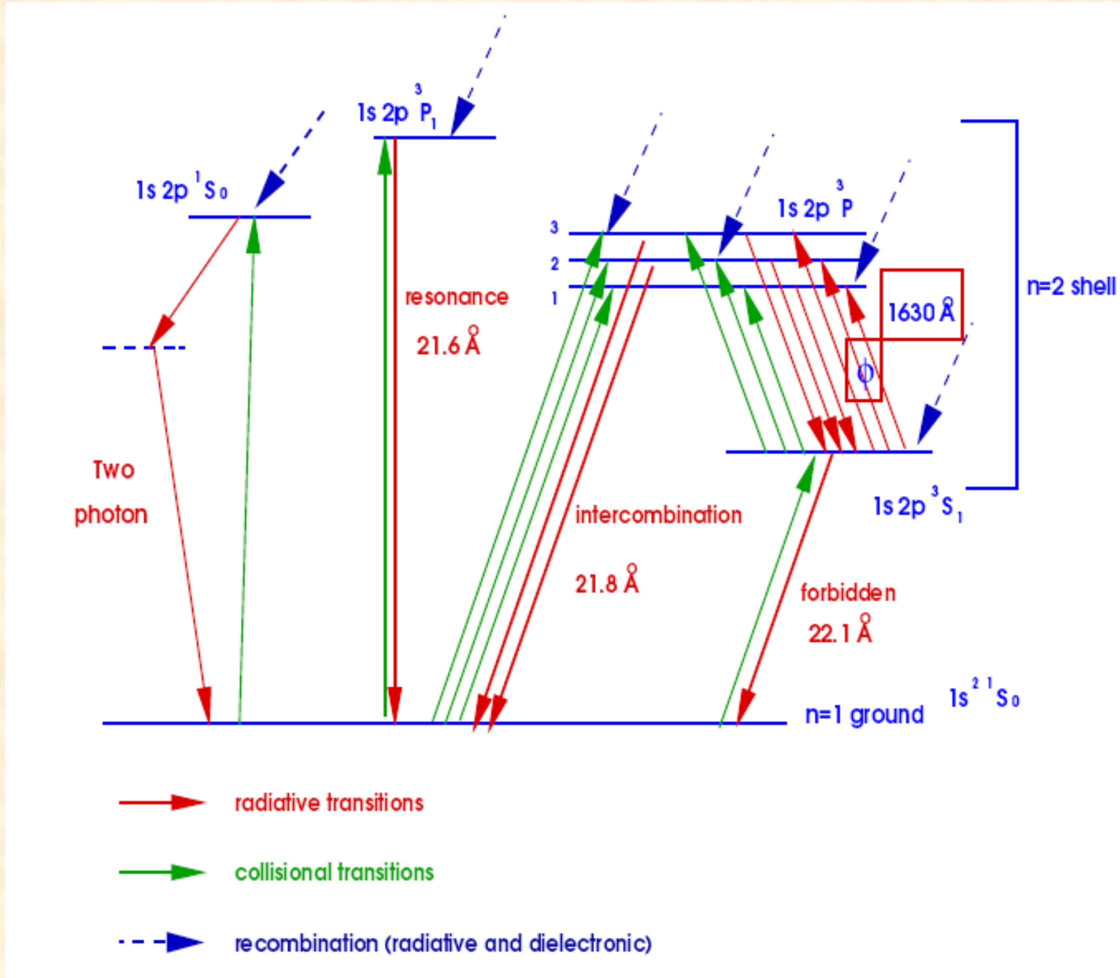


(Morales 2002)

- Triplet lines are sensitive to density, since the intercombination and forbidden lines can be collisionally de-excited.
- Unfortunately, the critical densities are rather high: $n_e \approx 10^{10}$ cm$^{-3}$, so not much help for the NLR (useful for higher density gas).

# High-Energy Processes - Inner Shell Ionization

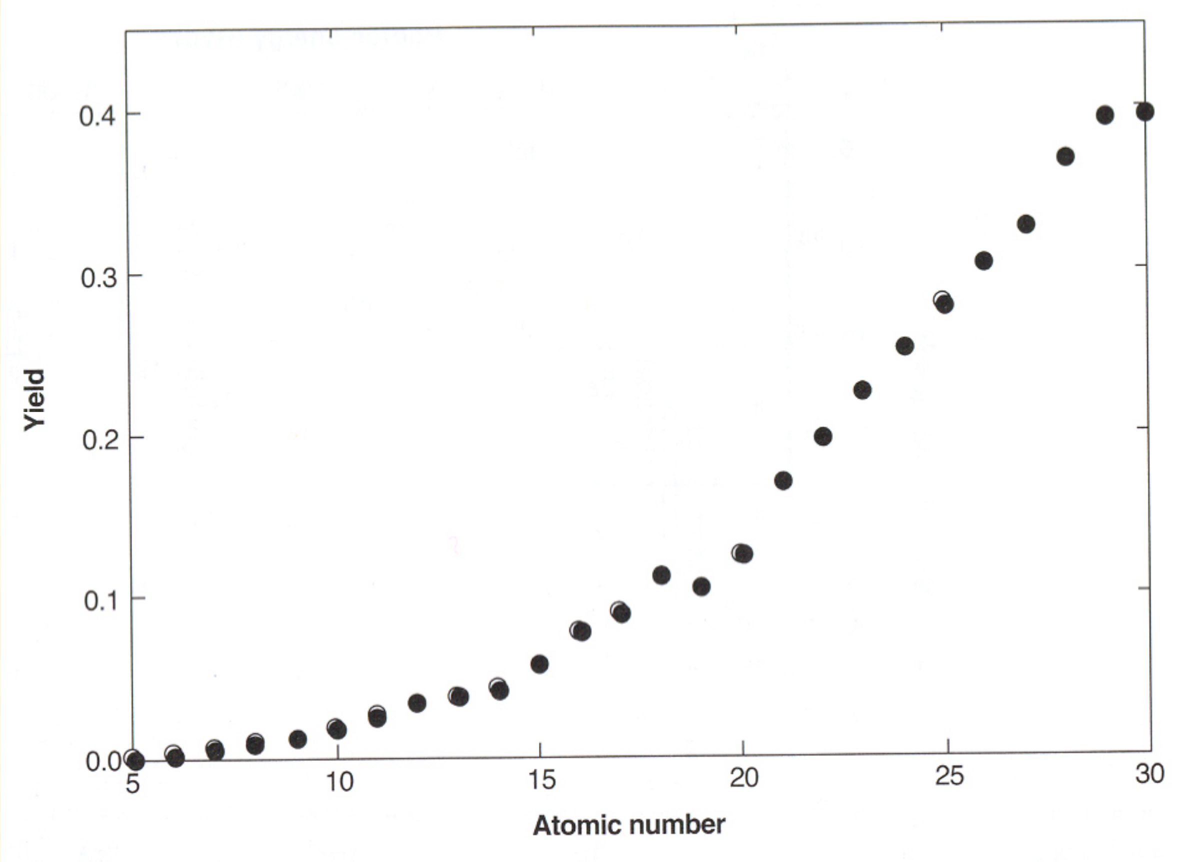


(Osterbrock & Ferland, p. 280)

- Inner shell ionization - vacancy filled by ejection of electrons (Auger effect) and/or fluorescent emission
- Yield = probability of filling K-shell vacancy by emission of Kα line.
- Fe (Z = 26) is abundant and has a high yield: Fe Kα is strong in hard X-ray region.

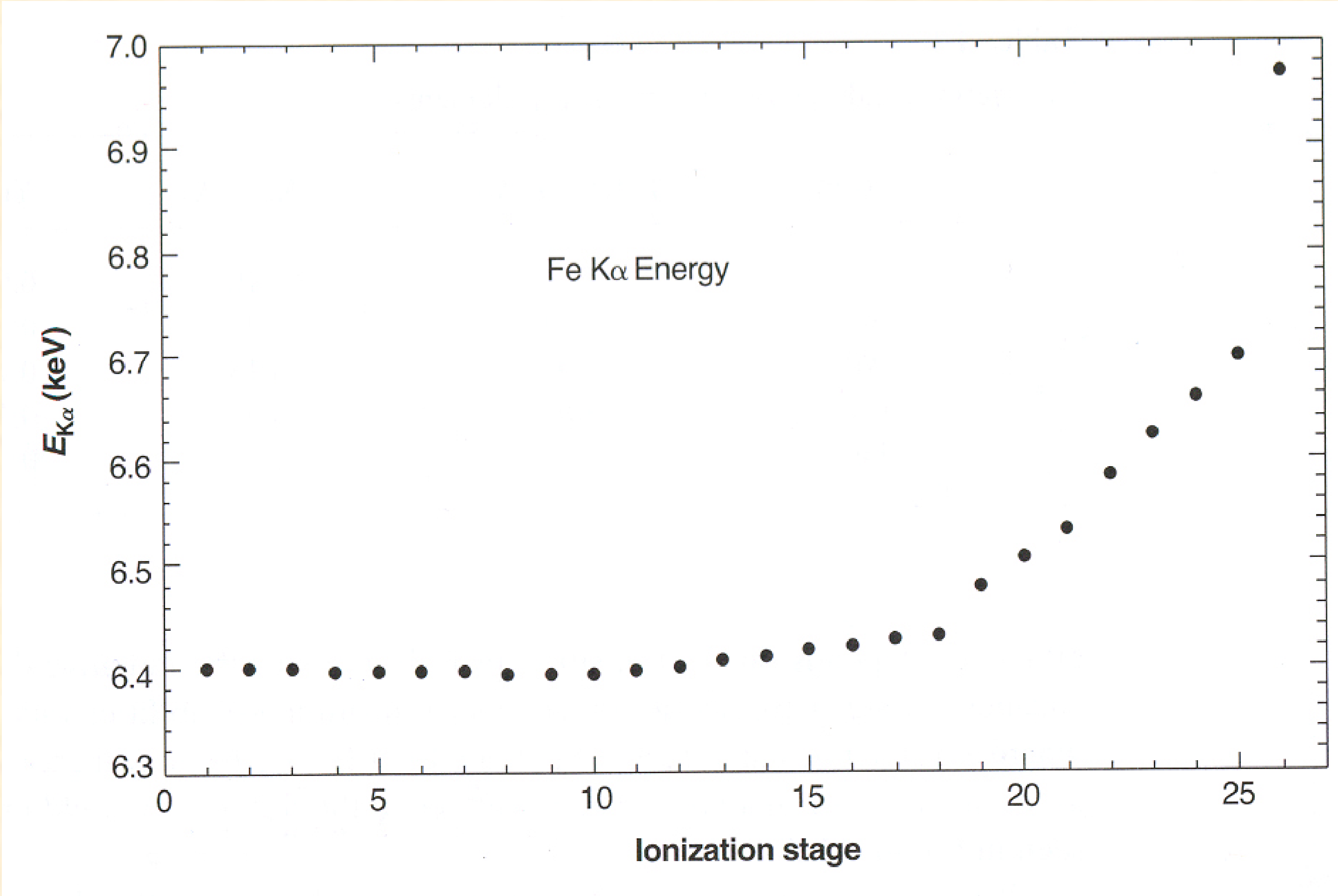


(Osterbrock & Ferland, p. 282)

- Energy of Fe Kα increases with ionization state, as there is less "screening" of nucleus by outer electrons with non-zero wave functions close in.
- With high-resolution spectroscopy, one can determine ionization state of gas from Fe peak (Fe XVIII and lower often known as "cold iron" by X-ray astronomers).

# Fe Kα Emission from MCG-6-30-15

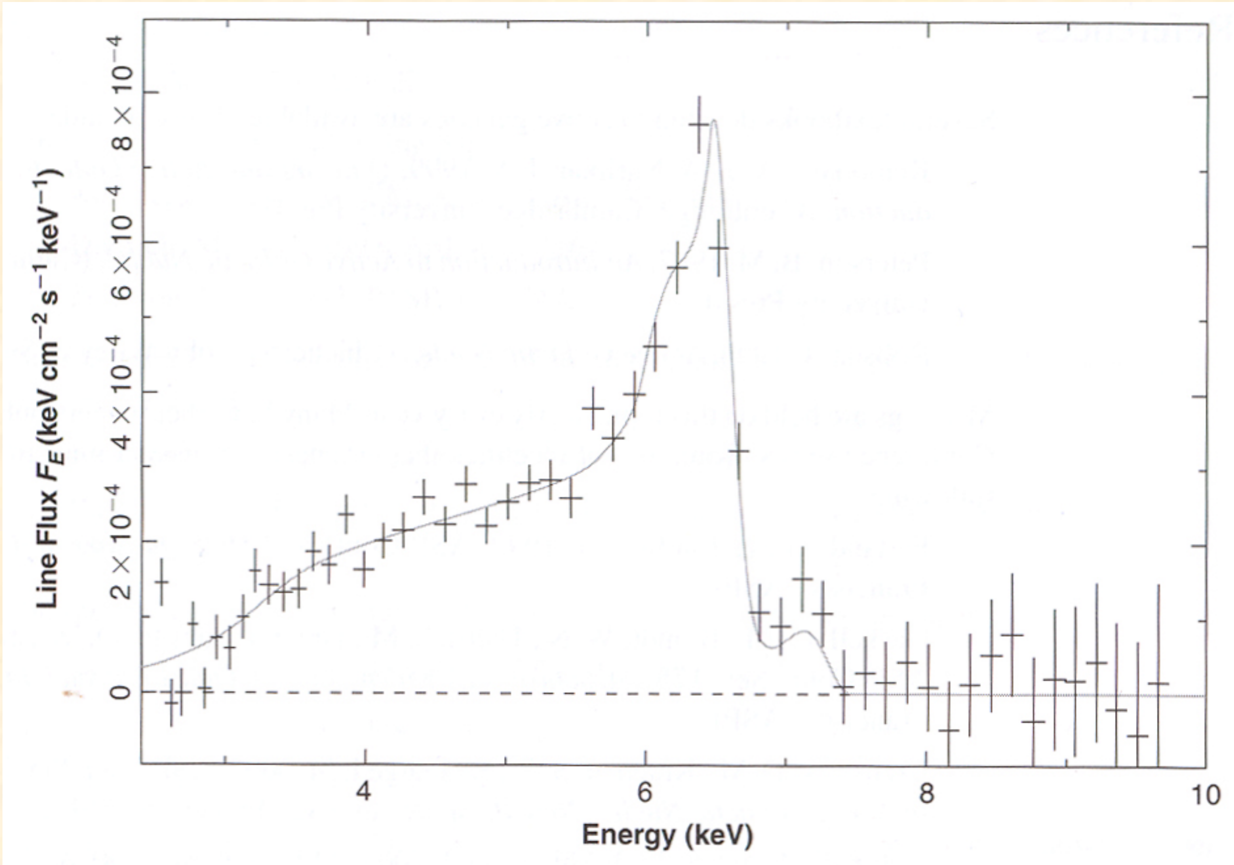


(Osterbrock & Ferland, p. 349)

- Relativistic disk fit to Fe Kα profile, velocity up to ~0.4c
- Rest-frame line center at 6.4 keV - consistent with emission from cold accretion disk.
- Peak slightly blueshifted due to Doppler boosting of approaching gas.
- Long red tail due to GR: can measure BH mass and spin.